nanoPaint: dynamic imaging of nanoscopic structural plasticity of the plasma membrane

Mariana Tasso[*]*, Thomas Pons, Nicolas Lequeux, Julie Nguyen, Zsolt Lenkei* and *Diana Zala*[*]

Materials. The materials required for the synthesis of the QD nanoparticles and of the QD ligand were as detailed in Tasso *et al.* (Tasso et al., 2015). Recombinant protein A (45 kDa) was purchased from ProSpec as a solution without additives. Bis(sulfosuccinimidyl)suberate (BS3) linker and Rabbit polyclonal anti-CB1 N-Ter antibody (PA1-743) were from Thermo Scientific. Mouse monoclonal anti-FLAG (IgG2) antibody was purchased from Sigma-Aldrich. Neurobasal™, B-27 and Lipofectamine®2000 Transfection Reagent, DMEM (Dulbecco's Modified Eagle Medium, high glucose, GlutaMAX without sodium pyruvate), Fetal Bovine Serum (FBS), penicillin-streptomycin (10,000 U mL^{-1}) and Trypsin-EDTA (0.05 %) phenol red were obtained from Life Technologies. Rabbit anti-N-terminal-CB1 antibody was produced by Double-X program (Eurogentec) as detailed in Leterrier *et al*. (Leterrier et al., 2004). High precision coverglasses (1.5H) were from Marienfeld Superior. Ludin Type 1 chambers were purchased from Life Imaging Services (Switzerland).

Quantum dot synthesis and ligand exchange. Red-emitting (λ_{em} = 650 nm) CdSe/CdS/ZnS multishell quantum dots were synthesized following published protocols (Yu and Peng, 2002; Li et al., 2003). Core/multishell QDs in hexane (4 nmol) were precipitated by ethanol addition followed by centrifugation (16,000 g, 5 min, unless otherwise stated). After supernatant's removal, QDs were mixed with 3-mercaptopropionic acid (MPA, 500 µL) using a sonicating bath and then stored at 60°C for 6–12 h. MPA-capped QDs were resuspended in 1 mL chloroform and thereafter precipitated by centrifugation. The obtained QDs were dissolved in ~1 mL DMF and precipitated by addition of ~50 mg of potassium *tert*-butoxide. The suspension was afterwards centrifuged to remove the basic organic supernatant and the nanoparticles washed twice with ethanol before redispersion in 400 µL of 100 mM sodium bicarbonate buffer (pH = 10.8). Thereafter, the block copolymer ligand (4 mg)

was resuspended in 100 mM sodium bicarbonate buffer (200 μL) and added to the MPA-QDs dispersion. The nanoparticles were left overnight at room temperature to complete the cap exchange. Free ligands were removed by two rounds of ultrafiltration (16,000 g, 10 min) in Vivaspin 100 kDa membrane filter units (buffer = 100 mM NaCl). Polymer-capped QDs were thereafter purified by ultracentrifugation (268,000 g, 25 min) in a 10%–40% sucrose gradient in 100 mM NaCl. The QD band was collected and sucrose removed by several rounds of ultrafiltration (100 kDa Vivaspin filter, 16,000 g, 10 min). The ligand-exchanged nanoparticles were finally resuspended in 600 μL of 50 mM HEPES, 100 mMNaCl, pH 7.5 and stored at 4°C in the dark.

Bioconjugation of the QD nanoparticles. Ligand-capped QDs (0.4 nmol) in 100 μL of 50 mM HEPES, 100 mM NaCl, pH 7.5 buffer were reacted for 30 min with 0.42 μmol of BS3 (50 mg mL^{-1} stock solution in DMSO; BS3 molar excess to QDs ~1000) under mixing in a rotating platform. Unreacted BS3 was afterwards removed via three rounds of membrane filtration (50 kDa Vivaspin filter, 16,000 g, 7 min) in 50 mM HEPES, 100 mM NaCl, pH 7 buffer and the linker-modified QDs resuspended in 100 μL of pH 7.5 buffer. Covalent binding of an intermediate protein A layer to the linker-modified QDs was performed by adding a 10× molar excess of protein A to the QD suspension and by letting the reaction proceed for 1 h under mixing in a rotating platform. Here, the total volume was adjusted to yield final QD concentrations of 3–4 μM. After incubation, unreacted protein A was removed via two ultracentrifugation cycles (151,000 g, 25 min). QD-protein A (QD-pA) samples were thereafter resuspended in 100 μL of pH = 7.5 buffer and mixed with ~100 μL of buffer-exchanged antibody (Ab) (rinsing buffer = 50 mM HEPES, 100 mM NaCl, pH = 8.5 adjusted with 2 M NaOH aqueous solution) at a 1:4 QD:Ab ratio. The antibody binding reaction to the QD-pA nanoconstructs was left to evolve for 1h under mixing in a rotating platform. Mouse anti-FLAG (IgG2) and rabbit anti-CB1 N-Ter antibodies were used. Unbound Ab was not removed and the QD-pA-Ab conjugates (~1–1.5 μM) were stored at 4°C until use without the addition of preservatives or other compounds.

Neuronal culture. Rat hippocampal neuronal cultures were obtained and cultured as described in Leterrier*et al*. (Leterrier et al., 2004). Briefly, hippocampi of rat embryos were dissected at embryonic days 17–18, trypsinized and dissociated with a Pasteur pipette. For epifluorescence tests, cells were plated on poly(-D-lysine)-coated coverslips at a density of 50,000 cells per 18 mm coverslip and cultured in complete Neurobasal™ medium supplemented with B27, 0.5 mM L-glutamine, 10 U mL^{-1} penicillin G and 10 mg mL^{-1} streptomycin. This medium was conditioned incubating glial cultures for 24 h. Transfection was performed at DIV8 (days *in vitro*) with Lipofectamine 2000 according to the manufacturer's instructions. The following plasmids were used: FLAG-CB1-GFP(Leterrier et al., 2006) and tdtTomato-Bassoon (Matz et al., 2010). For super-resolution imaging, the use of 18 mm high precision coverglasses was the sole difference with the epifluorescence procedure detailed above. Immunostaining of the CB1 receptor was carried out with a home-made rabbit anti-N-terminal-CB1 antibody (Leterrier et al., 2004) as primary and anti-rabbit Alexa488 as secondary antibody.

HEK cell line culture. Stable HEK cell line expressing FLAG-CB1-GFP was cultured in DMEM GlutaMAX supplemented with 10 vol.% fetal bovine serum and 1 vol.% of 10,000 U mL^{-1} penicillin-streptomycin.

QD incubation and video microscopy. Coverglasses were mounted in a Ludin Type 1 chamber wherein 900 µL of video microscopy medium (20 mM NaCl, 3 mM KCl, 10 mM HEPES, 2 mM $CaCl_2$, 2 mM $MgCl_2$, 10 mM D-glucose, 2 vol.% B27) at 37 °C was added. The chamber was thereafter placed in a Nikon Eclipse Ti inverted microscope (Nikon Instruments) equipped with a microscope stage incubator (Okolab, Italy) and an Apo TIRF 100×H 1.49 objective. To the 900 µL, 100 µL of the QD bioconjugates' suspension in warm (37 °C) video microscopy medium was added (final QD concentration in the Ludin chamber: 1–3 nM) and followed by ~5 min incubation. For

epifluorescence experiments, QD suspension was removed and replaced by fresh, warm video microscopy medium. Images were acquired under conventional FITCH and TexasRed® excitation/emission filter combinations (Nikon Intensilight mercury light source). For the super-resolution microscopy runs, QDs were not removed, thus remaining available in the solution. Samples were continuously illuminated with a 405 nm laser source (5–10% power) and images were acquired with an iXon3 back-illuminated EMCCD camera (Andor, Oxford Instruments) at 67 Hz. To overcome the blinking of QDs, we have simply extended the time frame for each data acquisition without compromising resolution. Given the high photostability of QDs, extended time-lapse imaging is feasible without affecting their brightness. To facilitate the localization of single emitters in a given ROI, we have tuned the density of QDs in the sample working mostly with a few QDs per ROI. Cumulative and/or time-lapse images were constructed by overlapping QD's localizations over time. Typically, 5,000–30,000 frames were recorded. A scarce number of QDs unspecifically adsorbed to the glass coverslip were employed as fiduciary markers for image correlation and drift correction.

Data analysis. Video microscopy images were processed with the Fiji software (ImageJ) (Schindelin et al., 2012). ThunderSTORM ImageJ plugin (Ovesný et al., 2014) was used for the localization of single particles as well as for image reconstructions. Because we do not ambition to individualize single particle trajectories but to cumulate them into a 3D topographical map, there is no need to correct for overlapping trajectories nor to discard interrupted trajectories. Kymographs were generated with a home-made plugin, KymoToolBox (Zala et al., 2013).

Reconstructed surface fraction and diffusion coefficient calculations. QD Brownian motions were simulated to understand the influence of the diffusion coefficient on the reconstructed area and reconstruction speed. For each set of parameters, 50 different Brownian trajectories were simulated on flat 2D surfaces. QDs were located with a +/- 10 nm accuracy at a 62 fps rate, corresponding to 16 ms per image. Each trajectory provided A_1, the area covered by the 20x20 nm dots symbolizing

each QD position at 16 ms intervals. The reconstructed surface fraction f is then given by $f = 1 - e^{-dA_1}$, where d is the QD surface density.

Supplementary Figures

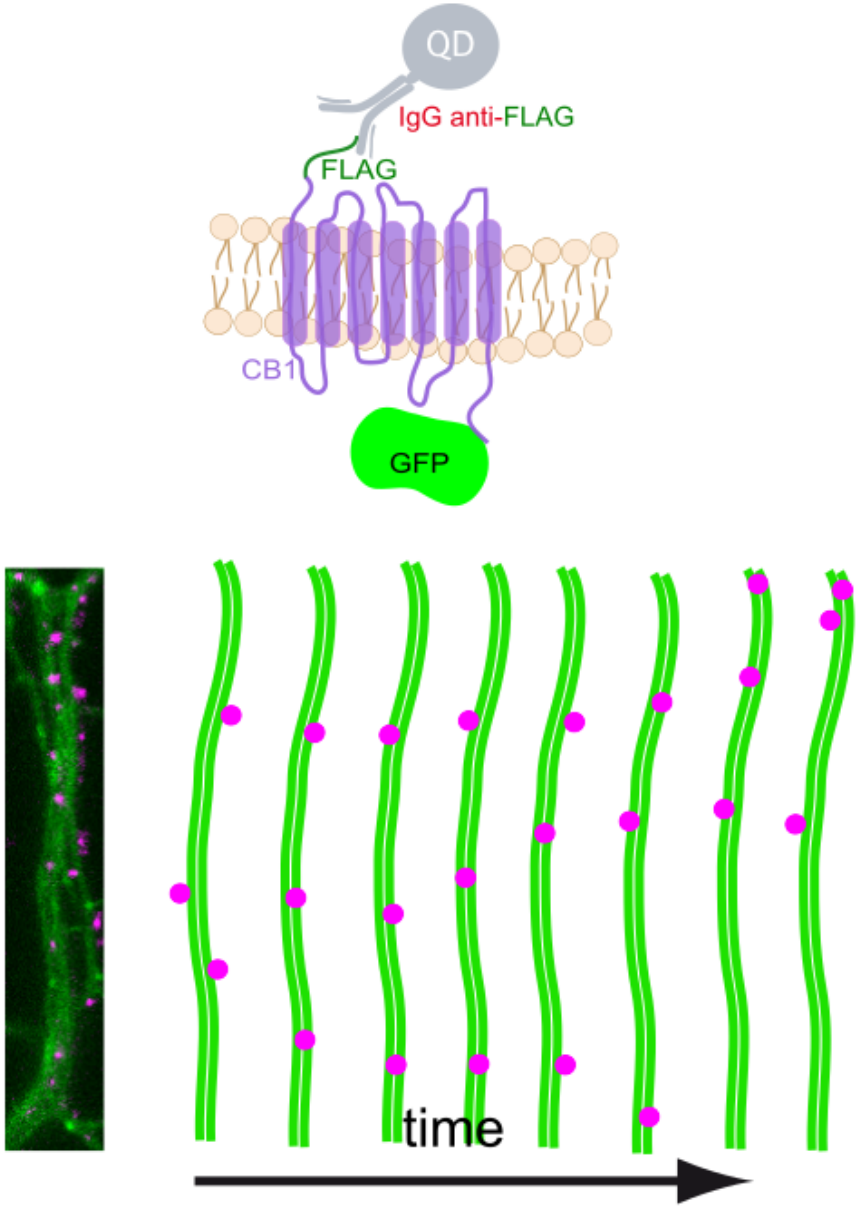

Figure S1: Conceptual scheme of a typical single-particle experiment recording GFP and QD signals: cells expressing the FLAG-CB1-GFP receptor were incubated for 5 minutes with biofunctional QD-pA-anti-FLAG nanoconstructs. The fluorescence image (down left) shows the continuous GFP (green) signal at the membrane with sharper, dot-like signals coming from GFP

vesicles and also the QDs attached to a few receptors (magenta dots). The cartoon (down right) illustrates the dynamics of receptor movement that can only be observed with QDs while the collective dynamics (GFP) appears static.

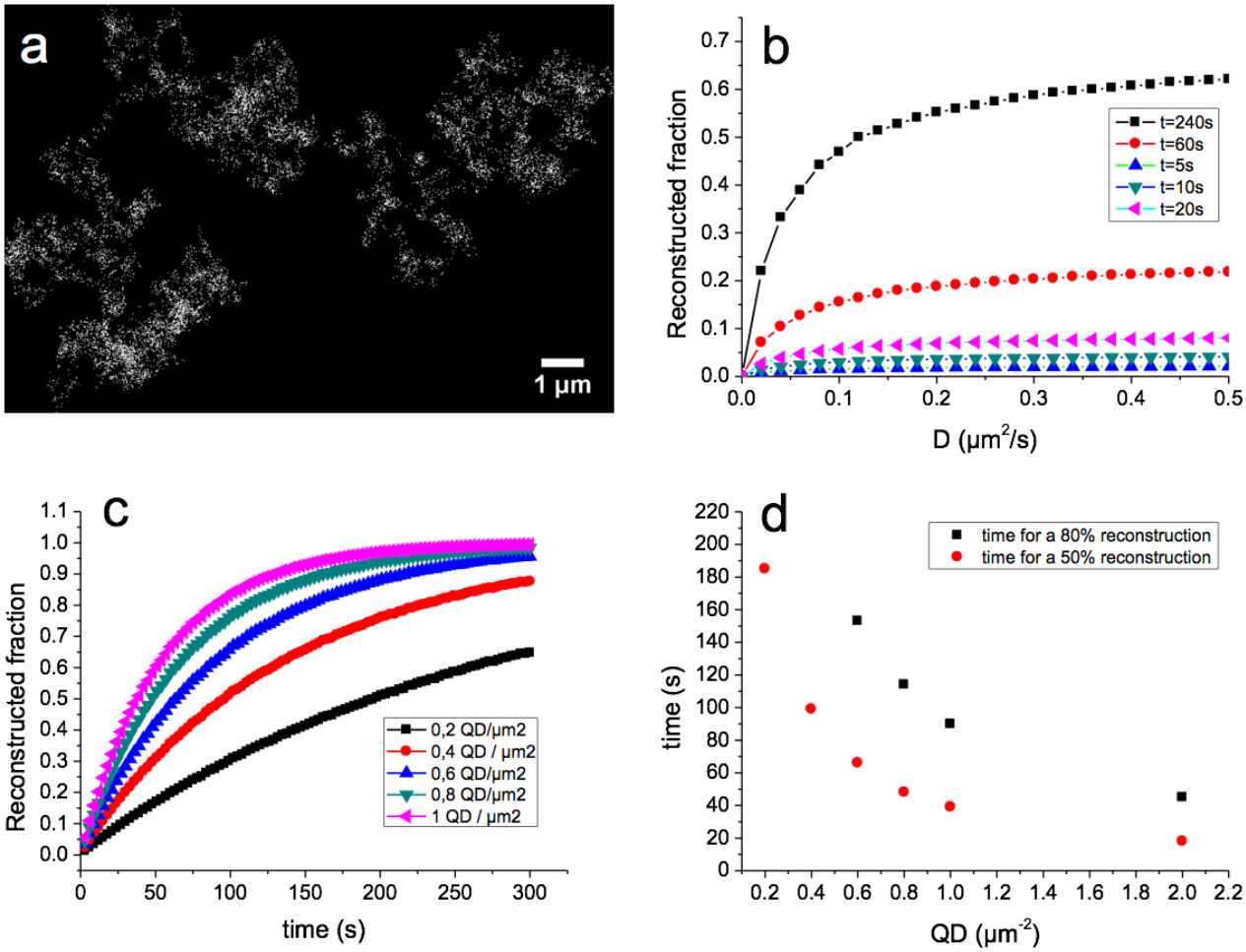

Figure S2: Simulations of 2D Brownian motions for QDs. A) Example of a 240 s simulated 2D trajectory with 62 points per second, D = 0.5 $\mu m^2 s^{-1}$, and a resolution of 20x20 nm^2 per point. The total reconstructed area for this trajectory corresponds to 4.88 μm^2; B) Average surface fraction reconstructed as a function of diffusion coefficient and for different trajectory reconstruction times, assuming a QD density of 0.2 μm^{-2}; C) Average surface fraction reconstructed as a function of time, assuming D = 0.19 $\mu m^2 s^{-1}$, and for different QD densities. D) Time necessary to reconstruct 50% or 80% of the surface as a function of QD density, assuming D = 0.19 $\mu m^2 s^{-1}$. Not shown in the graph is the time for 80% reconstruction at 0.2 μm^{-2}, which is of 460 s.

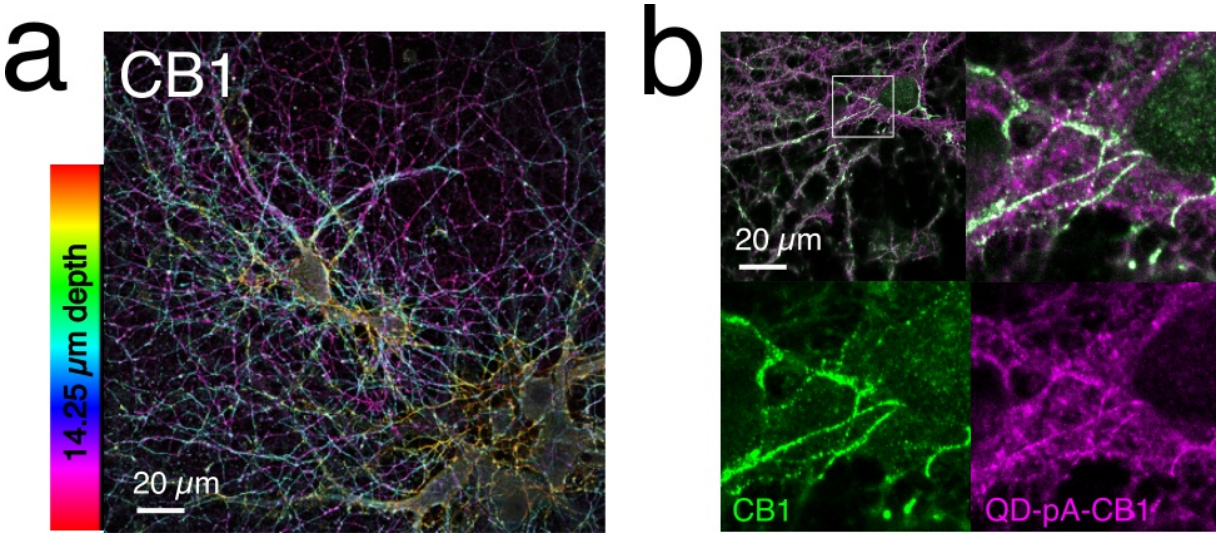

Figure S3: QDs on endogenous CB1 receptor. (a) Projection of a z-stack of confocal images of hippocampal rat culture cells immunostained for endogenous CB1; the color code encodes the depth. (b) Cultures were incubated with QD-pA-anti-CB1 nanoconstructs before processing for immunostaining with an anti-CB1 antibody. In the upper panel, the montage shows the overlay between the CB1 (green) and the QDs (violet) channel, both in wide field (left) and in a zoomed-in region (left). In the lower panel, CB1 and QD channels corresponding to the zoomed-in region.

Supplementary Movies

Video S1: Time-lapse of hippocampal neurons expressing FLAG-CB1-GFP (green) incubated for 5 minutes with biofunctional QD-pA-anti-FLAG nanoconstructs (magenta) (Figure 1c,d is related to this video).

Video S2: 3D projection of temporal integration of QD localizations around a presynaptic terminal (Figure 3 is related to this video).

References

Leterrier C, Bonnard D, Carrel D, Rossier J, Lenkei Z (2004) Constitutive Endocytic Cycle of the CB1 Cannabinoid Receptor. J Biol Chem 279:36013–36021.

Leterrier C, Laine J, Darmon M, Boudin H, Rossier J, Lenkei Z (2006) Constitutive activation drives compartment-selective endocytosis and axonal targeting of type 1 cannabinoid receptors. J Neurosci 26:3141–3153.

Li JJ, Wang YA, Guo W, Keay JC, Mishima TD, Johnson MB, Peng X (2003) Large-Scale Synthesis of Nearly Monodisperse CdSe/CdS Core/Shell Nanocrystals Using Air-Stable Reagents via Successive Ion Layer Adsorption and Reaction. J Am Chem Soc 125:12567–12575.

Matz J, Gilyan A, Kolar A, McCarvill T, Krueger SR (2010) Rapid structural alterations of the active zone lead to sustained changes in neurotransmitter release. Proc Natl Acad Sci 107:8836–8841.

Ovesný M, Křížek P, Borkovec J, Svindrych Z, Hagen GM (2014) ThunderSTORM: a comprehensive ImageJ plug-in for PALM and STORM data analysis and super-resolution imaging. Bioinformatics 30:2389–2390.

Schindelin J, Arganda-Carreras I, Frise E, Kaynig V, Longair M, Pietzsch T, Preibisch S, Rueden C, Saalfeld S, Schmid B, Tinevez J-Y, White DJ, Hartenstein V, Eliceiri K, Tomancak P, Cardona A (2012) Fiji: an open-source platform for biological-image analysis. Nat Meth 9:676–682.

Tasso M, Giovanelli E, Zala D, Bouccara S, Fragola A, Hanafi M, Lenkei Z, Pons T, Lequeux N (2015) Sulfobetaine–Vinylimidazole Block Copolymers: A Robust Quantum Dot Surface Chemistry Expanding Bioimaging's Horizons. ACS Nano 9:11479–11489.

Yu WW, Peng X (2002) Formation of High-Quality CdS and Other II–VI Semiconductor Nanocrystals in Noncoordinating Solvents: Tunable Reactivity of Monomers. Angew Chemie Int Ed 41:2368–2371.

Zala D, Hinckelmann M-V, Yu H, Lyra Da Cunha MM, Liot G, Cordelières FP, Marco S, Saudou F (2013) Vesicular glycolysis provides on-board energy for fast axonal transport. Cell 152.